J Mater Sci (2008) 43:2686–2692
DOI 10.1007/s10853-007-2415-y

Wear behavior of WC_P/Fe–C composites under high-speed dry sliding

Song Yan-pei · Yu Hua · Mao Xie-Min

Received: 21 August 2007 / Accepted: 20 December 2007 / Published online: 19 February 2008

Abstract WC_P/Fe–C composites are manufactured by centrifugal casting method. Dry sliding wear behaviors of the composites containing about 70 vol.% of WC_P were investigated at room temperature against 3Cr2W8V die steel counter face. And wear experiments were performed under loads of 50, 100, 150, and 200 N and sliding velocities of 20, 40, 60, and 80 m/s. Results showed that at the low load of 50 N, the composites, under different sliding velocities, all displayed significantly superior wear resistance. Meanwhile the results also showed that the variation of wear weight loss and wear rate of the composites was almost linear with sliding velocity when the sliding velocity and the load were below 60 m/s and 100 N. But as the sliding velocity and the load exceed 60 m/s and 100 N, the weight loss and wear rate of the composites increased rapidly. But the effect of the load applied on wear weight loss and wear rate was larger than that of the sliding velocity. Finally, the mechanism of the dry sliding wear is discussed in the article.

S. Yan-pei (✉) · Y. Hua
School of Material Science and Engineering, Henan University of Science and Technology, 471003 Luoyang, China
e-mail: sypei@mail.haust.edu.cn

Y. Hua
e-mail: kedayuhua@126.com

M. Xie-Min
School of Material Science and Engineering, Shanghai University, 200072 Shanghai, China
e-mail: xmmao@sh163.net

Introduction

As seen earlier, the working conditions of the roller ring used in high-speed wire or rod mill are very severe, so a series of requirements for the roller ring have to be fulfilled. A high wear-resistant surface layer of the roller ring is required. Meanwhile a ductility core matrix is also needed for the roller ring used in high-speed wire or rod mill. In recent years, a hard alloy fabricated by powder metallurgy (P/M) has been employed in the roller ring. It has excellent abrasive wear resistance and high abilities to withstand the abrasive impact and gall at elevated temperatures and high speeds. However the hard-alloy roller ring is more expensive and more difficult to make which restricts its application only for more small-sized-roller rings.

Particles-reinforced metal matrix composites as a heat-resistant wear-resistant material have been paid increasingly more attention, owing to low cost and good synthetic mechanical properties as well as physical properties [1]. The iron-based composites reinforced with particulate carbides (WC_P, VC_P), which improve their properties [2–4], have become the choice material to be used in the roller ring working at high-speed wire or rod mill. In this article, the wear behavior of the iron matrix composites reinforced with WC_P is investigated, and the mechanism of the dry sliding wear is discussed.

Experimental procedure

The matrix alloy of the WC_P/Fe–C composites was melted in an induction furnace of middle frequency. The chemical composition of the matrix alloy is given in Table 1. The reinforcement of the WC_P/Fe–C composites, i.e. tungsten

Table 1 Chemical composition of the Fe–C alloy

Elements	C	Si	Mn	Mo	Ni	Mg	Re	Fe
Wt%	3.2–3.6	2.4–2.8	<0.4	0.2–0.5	5.0–7.0	0.03–0.05	0.04–0.07	Remainder

carbide particle (WC_P), was commercially provided. The sizes of WC_P are 100–150 μm, the hardness of the WC particle is HRA93-93.7, the density is 16.5 g/cm^3, and the fusion temperature is 2,525 °C. Its chemical composition is given in Table 2. At 1,500 °C the mixture of the melted matrix and the preheated WC_P was poured into a mold which was rotating at 1,000–1,400 rpm. A thick-walled ring of WC_P/Fe–C composites, with dimensions of outer diameter 164 mm, inner 78 mm, height 68 mm, was obtained.

Metallographic specimens of size Φ14 × 20 mm were sectioned from the outer layer of the thick-walled ring along radius direction, and the surface was polished with an emery paper and a polishing cloth containing alumina dispersion. Determination of volume fraction had been carried out. The hardness of the composite layer was measured using an HR150D hardness tester. The microstructures of the WC_P/ Fe–C composites were analyzed by an optical microscope.

The experiments were performed under dry sliding wear conditions at a room temperature of 30–33 °C. Dry sliding wear behavior of the composites was investigated using a high-velocity wear testing machine which employed a steel ring rotating against the test pin held by a load applied. The weight loss of the test pin was determined at definite time intervals. The steel ring was made of 3Cr2W8V die steel, hardened to HRA76, and had a diameter of 160 mm (Fig. 1a). The size of the test pin is shown in Fig. 1b. The steel ring and the test pin were mounted on the testing machine, and the desired load was applied after the ring shaft was made to move at a given rotating speed. After the tests, they were cleaned and weighted at a scale with an accuracy of 10^{-4} g, and the change in pin weight loss with sliding velocity for a given time and load is recorded. These data are subsequently used in the calculation of wear rates presented in the results section of the article. The worn surfaces of the pins were examined using a JSM-56E scanning electron microscope and an energy-dispersive X-ray analyzer.

Table 2 Chemical composition of WC_P[11]

Code name	Tungsten (%)	Total carbon (%)	Free carbon (%)	Chloride (%)
YZ	95–96	3.7–4.2	0.1	<0.25

Results

The physical characteristics of the WC_P/Fe–C composite, fabricated by centrifugal casting route, are given in Table 3. The density of the composites varies from 11.6 to 10.3 g/cm^3, it means that a high amount of WC_P is obtained in the composites, because the density of WC_P is 16.5 g/cm^3 and the density of the ferrous alloy is 7.6 g/cm^3. The measured result shows that the volume fraction of WC_P in the composites is about 70 vol.%.

Figure 2 shows the microstructures of the composites observed under SEM at a magnification of 100× and 1000×, respectively. It is evident from Fig. 2 that WC_P composites are well distributed and are partially dissolved in the matrix (Fig. 2b).

Table 3 Physical characteristics of WC_P/Fe–C composites

Composite number	Volume fraction of WC particles (vol.%)	Hardness (HRA)	Density (g/cm^3)
WC_P/Fe–C composites	About 70	81	11.6–10.3

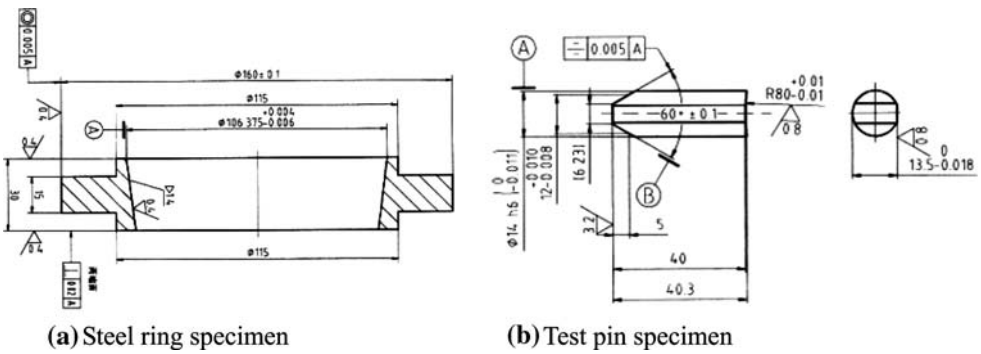

Fig. 1 Steel ring and test pin specimens

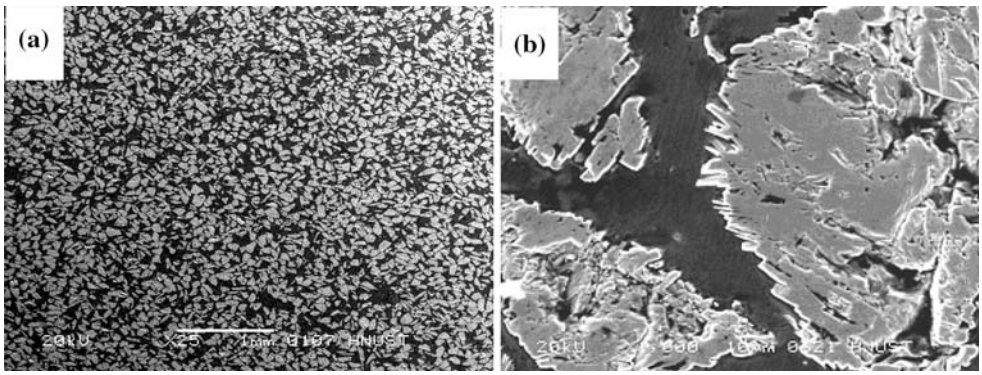

Fig. 2 Microstructures of WC_P/Fe–C composites layer fabricated by centrifugal casting, (**a**) WC_P distribution in the composite layer 25×, (**b**) WC_P of being dissolved partially 1000×

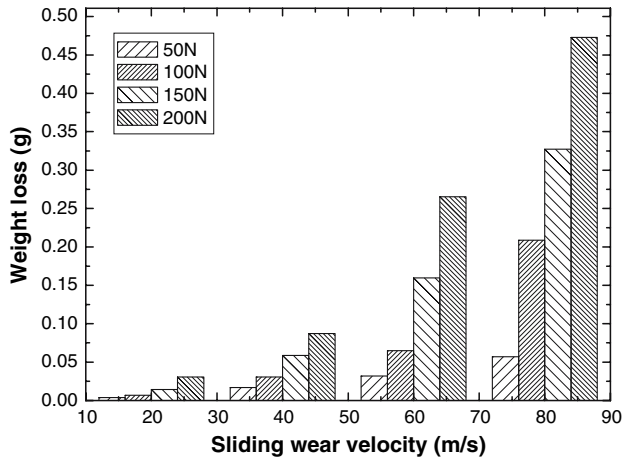

Fig. 3 Variation of wear weight loss with sliding velocities for WC_P/Fe–C composites under different loads

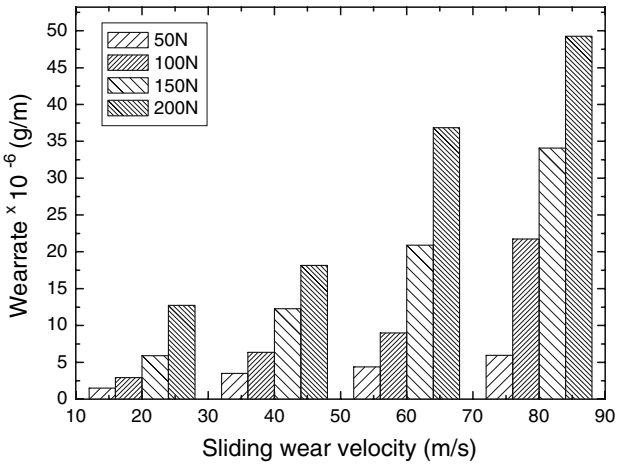

Fig. 4 Variation of wear rates with loads for WC_P/Fe–C composites under different sliding velocities

The composites containing about 70 vol.% of WC_P have been tested for dry sliding against a counter face of a steel ring of hardness HRC54. The variation of weight loss with sliding velocities is shown in Fig. 3, for tests carried out under loads of 50, 100, 150, and 200 N, respectively, and a fixed sliding time of 2 min. It is also observed that the wear weight loss of the composites almost linearly increases with the sliding velocity when the sliding velocity is below 60 m/s, and the weight loss increased rapidly when the velocity is over 60 m/s.

Figure 4 shows the variation of wear rate with load applied in the composite pin under different sliding velocities. It has been observed that the wear rate increases with loads applied at different sliding velocities. It is also known from Fig. 4 that except at the speed of 80 m/s, wear rates below loads of 100 N are smaller. When the given load increases up to 200 N, the wear rate of the composites pin increases obviously with sliding velocities and reaches 12.73×10^{-6}, 18.15×10^{-6}, 36.85×10^{-6}, and 49.26×10^{-6} g/m, respectively. But when the given load is reduced to 50 N, the wear rate under different sliding velocities is relatively smaller for the composites and reaches 1.48×10^{-6}, 3.5×10^{-6}, 4.4×10^{-6}, and 5.95×10^{-6} g/m, respectively.

Figure 5 shows the variation of friction coefficient with sliding velocities and applied loads for the composites at a sliding time of 120 s. It is observed that under testing loads, the friction coefficient of the composites at the sliding velocities of 20 and 40 m/s has a smaller variation and

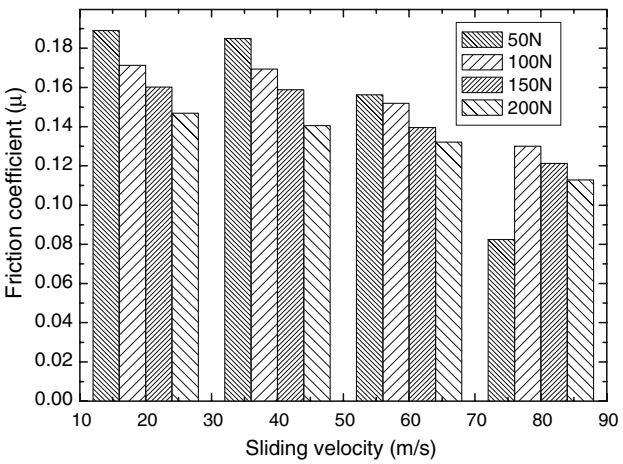

Fig. 5 Friction coefficient for WC_P/Fe–C composites at different loads and sliding velocities

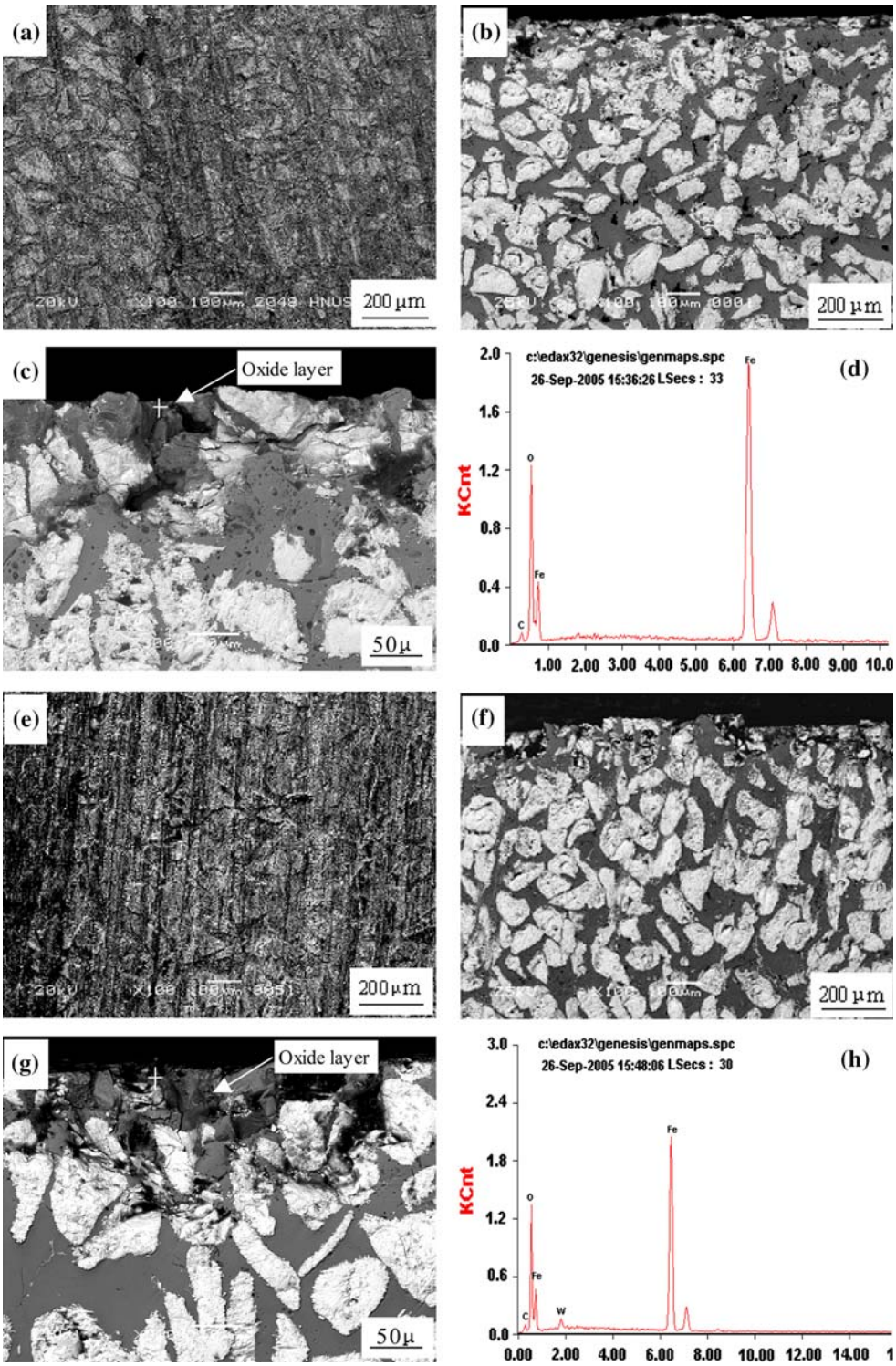

Fig. 6 Wear morphologies and EDX analysis of the composite pins worn surface run under a sliding velocity of 20 m/s and different loads (**a**)–(**d**) at a load of 50 N and (**e**)–(**h**) at a load of 200 N

reaches 0.189, 0.173, 0.1602, 0.1429 and 0.185, 0.1694, 0.1588, 0.1406, respectively. And when the sliding velocity is further increased up to 80 m/s, the friction coefficients of the composites with sliding velocities are obviously decreased. But when the sliding velocity increases up to 80 m/s, the coefficient of friction for the composites at the load of 50 N reaches a minimum value (0.0825). It is also known from Fig. 5 that under the same sliding velocity, the composites exhibited a continuous decrease in the coefficient of friction with loads applied throughout the test.

Figures 6 and 7 show the wear morphologies and EDX analysis of the wearing surface of the composite pins tested

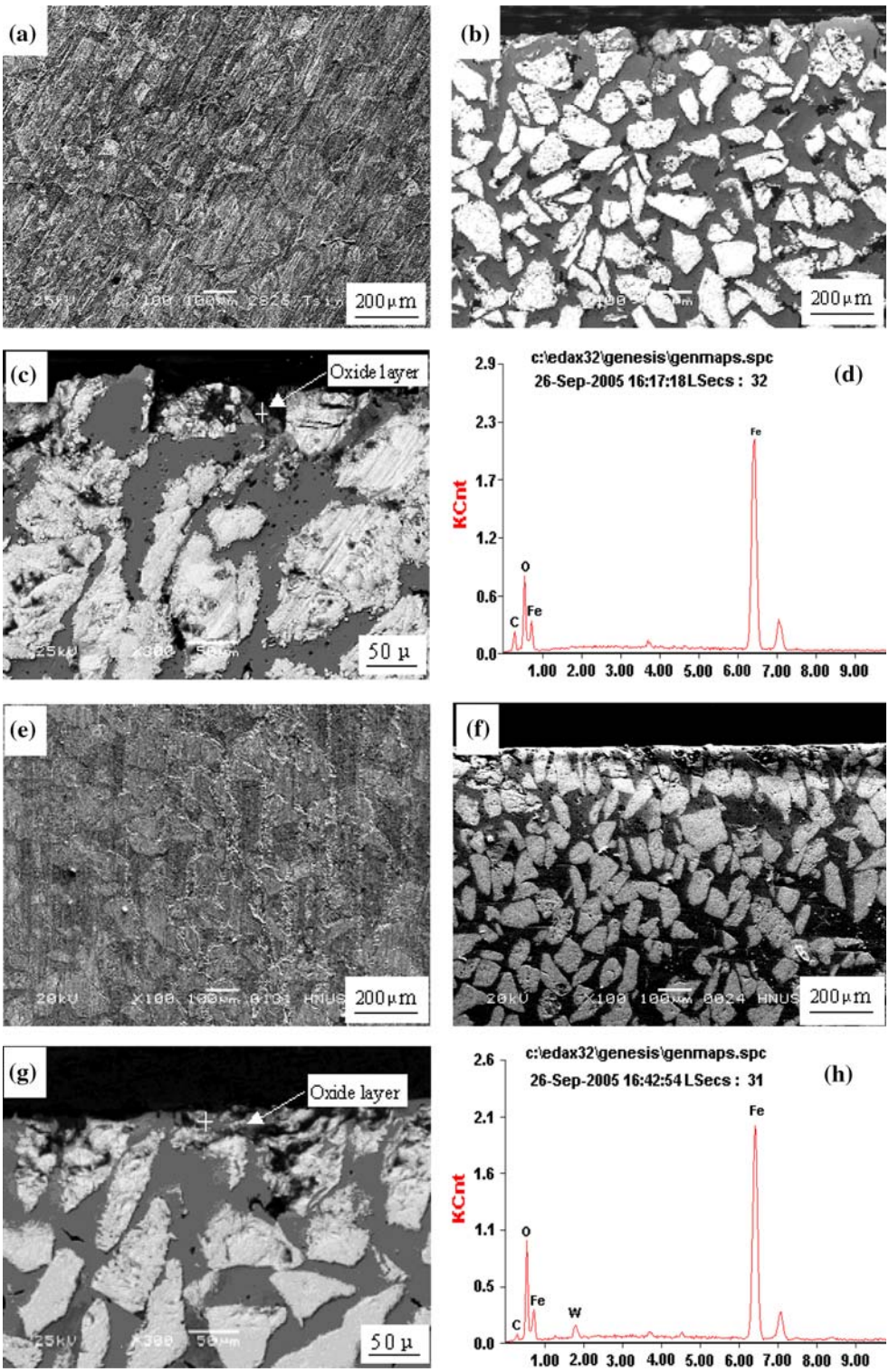

Fig. 7 Subsurface deformed layer and EDX analysis beneath the worn surface of the composite pins under a sliding velocity of 80 m/s and different loads (**a**)–(**d**) at a load of 50 N and (**e**)–(**h**) at a load of 200 N

at room temperature under the load of 50 N and different sliding velocities. The oxide layer present on the wear surface of the composites at the velocity of 80 m/s is much thinner than that observed on the same composites at the velocity of 20 m/s and is found to contain significant quantities of iron and oxygen.

It is observed from Figs. 6, 7 that under the tested conditions, a percentage of WC_P is retained at the wearing surface which does not undergo fracture and pull out. Examination of cross sections through the wear surfaces of composite pins tested at room temperature under the velocity of 20 m/s and two loads reveals a oxide material

layer is found in many places (see Fig. 6c, g), and the thickness of the oxide layer present beneath the worn surface of the composites at the load of 200 N is larger than that observed at the load of 50 N. These oxide regions beneath the worn surface consist almost exclusively of a mixture of iron oxide and broken WC_P (seen Fig. 6d, h). But when the sliding velocity increases up to 80 from 20 m/s, the oxide layer thickness beneath the worn surface of the composites under the same load is obviously reduced (seen Fig. 7c, d, g, and h).

Discussion

At the low levels of loading (50–100 N) and below the sliding velocity of 60 m/s, the composites reinforced with WC_P demonstrate better wear resistance. When the load and the sliding velocity are over 100 N and 60 m/s, wear resistance of the composites is obviously reduced. The temperature of the wear surface for the composite pin, below the load of 100 N and velocity of 60 m/s, is measured to be in the range of 294 to 657 °C. The lower temperature of the wear surface under low loads and sliding velocities slows down consequently the rates of oxide removal. And the smaller wear rate for the composite pin in the wear process is a direct result of the WC_P preventing metal-to-metal contact. When the sliding velocity increases up to 80 m/s, the temperature of the wear surface of the composite pin under different loads reaches over 800 °C. This will lead to generation of oxide films (high-temperature forms) on the wear surface of the composite pins, which are formed by the oxidation of the iron substrate itself. And the higher sliding velocity increases the rates of oxide removal and wear rate for the composite pin. Oxide films, discontinuous or otherwise, on the surface of steels had been reported to reach a critical thickness before breaking up to form wear debris [5]. This critical oxide thickness can vary enormously and can be in excess of 5 μm depending on its load-bearing capability. Vardavoulias [6] proposed that the size and the interfacial strength of the hard, reinforcement particles, and their relationship to the critical oxide thickness determine the rate mechanisms of wear in steel-based composite materials.

For the composite pin, the temperature of wear surface under low loads and sliding velocities is lower: consequently it slows down the rates of oxide formation and removal. The WC_P by preventing metal-to-metal contact at the wear surface, reduces the wear rate of the composites pin. Less metal-to-metal contact will also reduce the weight loss of the material being removed from the pin. Wear on WC particles that are strong at the surface at this time is low, but eventually they will be worn down, fractured, or stripped away together with the oxide around them and form stripped pits, leading to higher frictional coefficient (see Fig. 5). However, while the particles are retained at the surface, metal-to-metal contact cannot occur, and the oxide layer has a chance to regenerate through surface heating, allowing the whole process to start again.

The load-bearing capability of the material also has the effect of reducing the stress on the oxide layer, thus making it less likely to be removed. Under the same sliding velocity, the larger the applied load is, the higher the wear rate is (Fig. 4). When the given load increases up to 200 N, the temperature of the wear surface rises to over 800 °C. During this time, the iron oxides evolved at the wear surface are the high-temperature forms, i.e. Fe_3O_4. It acts as a solid lubricant to reduce the coefficient of friction. At higher loads and velocities, the stress on the oxide film becomes the influential factor for determining the wear rate. The higher wear surface temperature reduces the strength of the composite matrix, accelerates the oxidation of Fe–C matrix and the rate of the oxide film being removed, and increases thermal shock at the metal-oxide boundary and subsurface fatigue cracking. This pressure of high load would cause yielding of the iron matrix, which would result in WC_P being pushed below the wearing surface. Metal-to-metal contact makes oxide to grow rapidly, and the oxide film is fractured under the action of sliding (Fig. 7). Rapid wear occurred between the sample and the counter face. So the wear rate is increased.

Conclusions

The current study on the wear of Ferro–WC_P composites leads to the following conclusions:

- WC_P-reinforced iron matrix composites have been manufactured by centrifugal casting route, in which the distribution of WC_P is uniform, and composites containing about 70 vol.% of WC_P have been produced.
- Under dry sliding wear, the wear weight loss of the composites with sliding velocity is almost linear below the sliding velocity of 60 m/s, and the weight loss increases rapidly when the velocity is over 60 m/s.
- The composites' wear rate increases with sliding velocities and applied loads. When the loads applied increase up to 200 N from 50 N, the wear rate of the composites under different sliding velocities increases from 1.48×10^{-6}, 3.5×10^{-6}, 4.4×10^{-6}, and 5.95×10^{-6} g/m to 12.73×10^{-6}, 18.15×10^{-6}, 36.85×10^{-6}, and 49.26×10^{-6} g/m, respectively.
- The average coefficient of friction of the composites reinforced with WC_P exhibits a continuous decrease with the increase of applied loads and sliding velocities.

- Under the action of high-speed sliding wear, two regimes of wear are evident; (1) mild wear characterized by oxide generation and low wear rate and (2) severe wear characterized by metallic contact at the rubbing surfaces and high wear rate under high sliding velocities and loads.

References

1. Zhang SY, Meng FQ, Cheng YY (1996) Mater Rev 10(2):66
2. Kattamis TZ, Suganuma T (1990) Mater Sci Eng A 128:241
3. Rai VK, Srivastava R, Nath SK, Ray S (1999) Wear 231:265
4. Galgali RK, Ray HS, Chakrabarti AK (1999) Mater Sci Technol 15:437
5. Quinn TFJ, Sullivan JL, Rowson DM (1984) Wear 94:175
6. Vardavoulias M (1994) Wear 173:105